

Photothermal displacement measurement of transient melting and surface deformation during pulsed laser heating

Shaochen Chen and Costas P. Grigoropoulos^{a)}

Department of Mechanical Engineering, University of California, Berkeley, California 94720-1740

Hee K. Park and Pieter Kerstens

IBM Manufacturing Technology Center, Boca Raton, Florida 33431

Andrew C. Tam

IBM Almaden Research Center, San Jose, California 95120

(Received 15 June 1998; accepted for publication 11 August 1998)

A photothermal displacement method has been developed to probe the pulsed laser-induced transient melting and surface deformation of Ni-P hard disk substrates. A probing He-Ne laser beam is aligned collinearly with the near-infrared nanosecond pulsed heating beam. The He-Ne beam spot is scanned on the microfeatures formed on the sample surface by the pulsed laser heating. The deflection signals show the variation of the feature shape resulting from different pulse energies of the heating laser beam. The transient deflection signal also reveals that the time scale of the surface motion is in the range of several hundred nanoseconds. © 1998 American Institute of Physics. [S0003-6951(98)03141-6]

Laser-assisted melting and surface modification processes are important in a variety of industrial applications. A well proven technology to improve the stiction performance of hard disk drive for low-flying-height media is the laser zone texturing (LZT) of Ni-P hard disk substrates.¹⁻³ Several studies have reported the feature ('bump') formation upon pulsed laser irradiation,⁴ and the effect of the produced bump height on stiction performance.² It was found that the variation of substrate material, laser energy, or substrate surface preparation procedure would significantly affect the laser texture quality (bump shape and bump height).^{5,6} However, no attempt has been made to probe the physical process of bump formation during laser irradiation, even though it is recognized that catastrophic stiction failure occurs in the case where a produced bump height drops below a critical value.² It is the aim of this work to develop a noncontact photothermal displacement (PTD) technique to *in situ* diagnose the LZT process.

PTD has been developed to study material properties or to monitor various laser-induced surface phenomena.^{7,8} A position sensitive detector coupled with a lock-in amplifier is used to detect a minute deflection signal due to small temperature change or small thermoelastic deformation on the sample surface upon frequency-modulated laser heating in the thermoelastic regime.^{9,10} However, in the LZT process, the surface is permanently deformed due to melting after a single pulse heating. The bump diameter is usually from 5 to 20 μm and the height is in the tens of nanometers range, respectively. Moreover, conventional PTD setups are not technically practical to monitor the LZT process with the required stability and alignment reproducibility. Our goal is to develop a robust and high-resolution setup for measuring transient deformation on the material surface during single pulse laser heating. It is desired that the setup should have the capability of scanning the bump area, of distinguishing the bump shape change due to the heating beam energy

variation, and of monitoring the bump height variation in the nanometer range. This constitutes a new application of PTD in the study of transient melting and surface deformation in the short time regime and in small length scales upon pulsed laser heating. The technique can be applied to investigate transient surface phenomena in other laser materials processing applications.

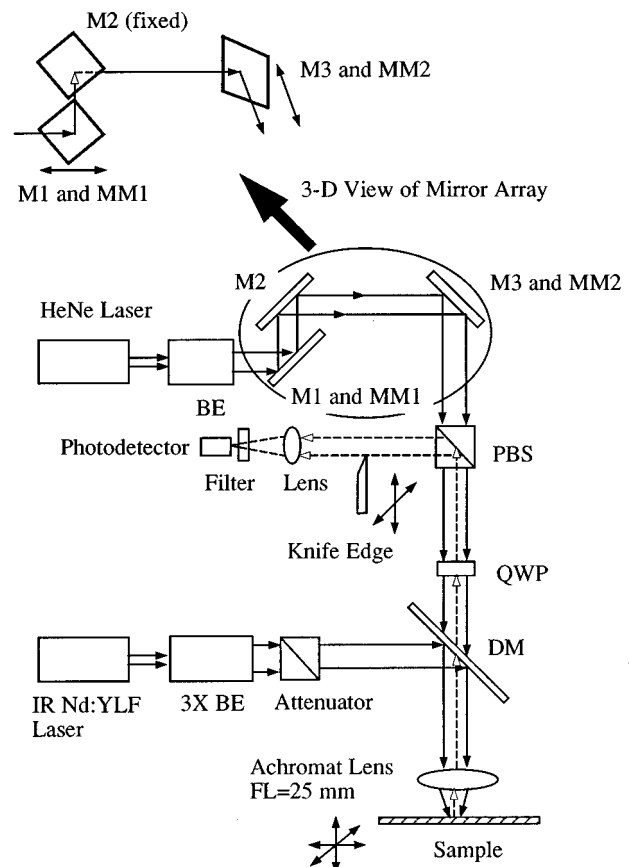


FIG. 1. Experimental setup for deflection and total reflection measurement. M: mirror; MM: micropositioning motor; BE: beam expander; PBS: polarizing beam splitter; QWP: quarter wave plate; DM: dichroic mirror.

^{a)}Electronic mail: cgrigoro@me.berkeley.edu

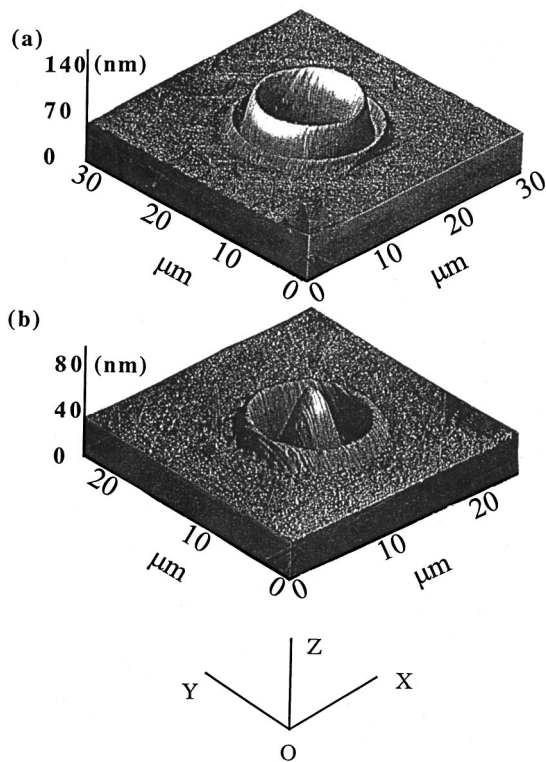


FIG. 2. Typical bump shapes in the LZT process depicting (a) a deep crater with a peripheral rim, (b) a central peak sombrero feature.

The experimental apparatus is schematically shown in Fig. 1. An infrared (IR) heating beam is emitted from a polarized Nd:YLF laser [$\lambda = 1047$ nm, full width half maximum (FWHM) = 15 ns], which is used for laser texturing of Ni-P hard disk substrates due to its good power stability. This beam is expanded by a $3\times$ beam expander. A cubic beam splitter is used to attenuate the laser intensity. The attenuated beam is then reflected through a dichroic mirror and finally focused onto a Ni-P substrate sample (12 wt. % P) by an achromat lens with an aperture of approximately 10 mm and focal length of approximately 25 mm.

The probing beam is a 20 mW linear polarized He-Ne laser ($\lambda = 632.8$ nm). It is expanded by a variable beam expander ($10\times\sim 20\times$). The expanded beam is reflected by three mirrors, passes through a polarizing beam splitter, a quarter wave plate, the dichroic mirror, and is focused onto the target surface by the achromat lens. The beam diameters for both beams are measured using knife-edge profiling. At the sample surface, the Nd:YLF laser beam diameter is approximately $17.2\ \mu\text{m}$ while the He-Ne laser beam diameter is about $4.8\ \mu\text{m}$ both at the $1/e^2$ intensity point. The depths of focus for the Nd:YLF and the He-Ne beams are about ± 70 and $\pm 10\ \mu\text{m}$, respectively. The achromat lens was designed for wavelengths of 1047 and 632.8 nm, allowing the focal points of these two beams to be positioned within $10\ \mu\text{m}$.

The reflected or deflected beam from the sample surface passes through the same dichroic mirror, the quarter wave plate, the polarizing beam splitter, a He-Ne interference filter, and is finally focused onto a photodetector. A knife-edge, cutting half of the reflected beam is used to obtain the deflection signal. The photodetector is connected to a digitizing

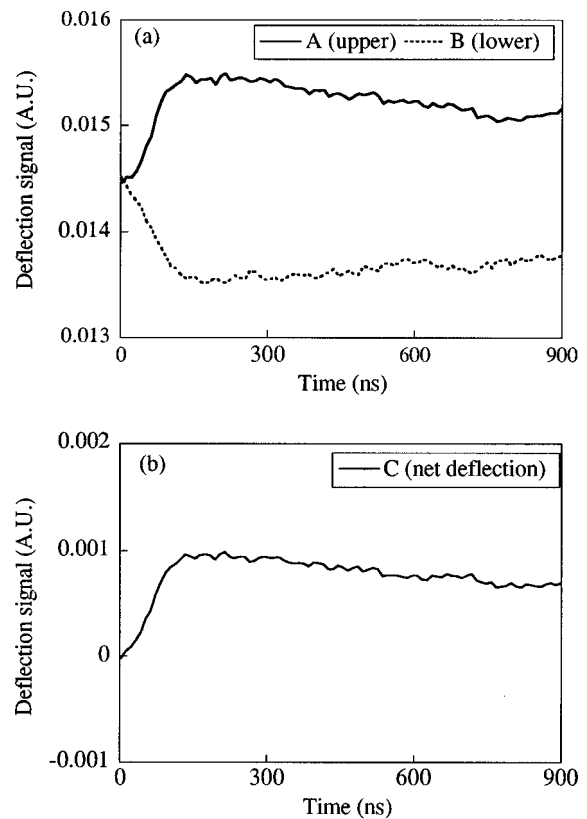


FIG. 3. (a) Deflection signal when the upper half reflected He-Ne beam is blocked (curve A), and deflection signal when the lower half reflected He-Ne beam is blocked (curve B), (b) real deflection signal due to surface deformation. The laser pulse energy is $3.2\ \mu\text{J}$.

oscilloscope (1 ns time resolution), which is triggered by the Nd:YLF laser pulse.

The probing He-Ne beam is aligned collinearly with the Nd:YLF laser beam. Rough alignment is first obtained by projecting the reflected He-Ne beam far away and viewing its scattering pattern after pulsing the heating beam. Further fine alignment is conducted by moving the mirrors, M1 and M3, which are mounted on two micropositioning motors. By moving M1 and M3, it is possible to scan the He-Ne beam over the sample surface in both the x and y directions. The micropositioning motor has a resolution of $1\ \mu\text{m}$. The travel of the two motors versus the movement of the probing beam on the sample surface is calibrated by using a knife edge. Since the texture feature produced by the Gaussian Nd:YLF laser beam is symmetric, its center has a minimum slope as shown in the atomic force microscopy (AFM) images displayed in Fig. 2. Hence, the center position of the He-Ne beam with reference to the heating beam on the sample surface is determined when the permanent deflection signal reaches minimum in both the x and y scanning directions.

Before measuring the deflection signal due to bump formation, the system is tested on a flat and untreated Ni-P sample. It is found that a very small slope (smaller than

The deflection signal is obtained as follows. First, the (about 0.2°) can be easily detected. For most cases in the LZT process, the bump (or crater wall) slope varies from 0.5° to 2° . He-Ne beam is moved $2\ \mu\text{m}$ away from the center of the Nd:YLF beam on the sample surface by the micropositioning motor. The knife edge shown in Fig. 1 is used to block the

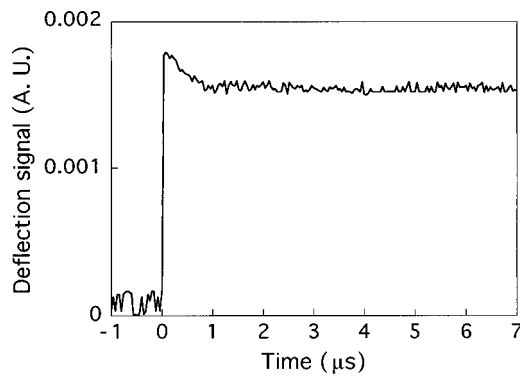


FIG. 4. Deflection signal in large time scale for laser pulse energy of 4.3 μJ .

upper half of the reflected He–Ne beam. No deflection signal can be detected if there is no surface deformation or surface temperature change. When a single pulse of 3.2 μJ energy is fired onto the surface, the surface is deformed and a bump is formed, causing the He–Ne beam deflection as shown in Fig. 3(a) (curve A). Then the knife edge is shifted to block the lower half of the He–Ne beam and another pulse is applied with the same energy to a new spot. Again, the reflected He–Ne beam is deflected as shown in Fig. 3(a) (curve B). By subtracting curve B from curve A and dividing the result by 2, the net deflection signal due to the deformation of the surface is deduced as shown in Fig. 3(b) (curve C). By adding curve B to curve A, the total reflection signal can be obtained. It is seen that the intrinsic surface reflectivity change during bump formation is small, which is in turn consistent with our previous study by fast multi-wavelength pyrometry.¹¹

The possible contribution from thermoelastic expansion to the deflection signal is also examined. The time scale of the thermoelastic response corresponding to pulsed deformation and the cooling period is in the several microseconds range.¹² However, as the transient deflection signal is ex-

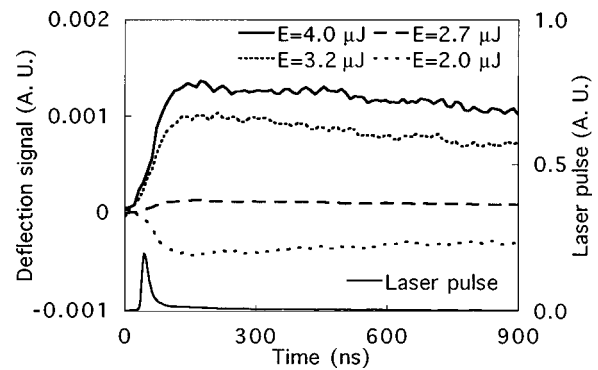


FIG. 6. Heating beam energy dependence of deflection signal.

tended from hundreds of nanoseconds to the microsecond time scale, the change in the magnitude of the deflection signal at long times ($t > 1 \mu\text{s}$) is very small (Fig. 4); confirming that the deflection is largely due to surface deformation and contribution from thermoelastic expansion is negligible. This figure also suggests that the motion of the deformed surface upon nanosecond laser heating is within several hundred nanoseconds, which is in agreement with the previous numerical study of bump formation.⁴ Moreover, the deflection signal does not exhibit an oscillatory temporal behavior, which is consistent with the thermocapillary driven outward flow in the crater formation, with the possibility of inward bulging flow for a range of laser parameters.

The dependence of the bump shape (measured by AFM) on the incident energy of the IR heating beam is shown in Fig. 5. When the incident heating beam energy is 4.0 μJ , the bump has a crater at the center and a low peripheral rim, while the bump attains a “sombbrero” shape when the laser energy is 2.0 μJ . The diameter of the bumps is about 17 μm , and the bump height varies from 50 to 10 nm. This change of the bump shape due to laser energy variation can be precisely identified in the probing beam deflection signals in Fig. 6. At heating beam energies exceeding 2.7 μJ , the deflection signal is enhanced, indicating a crater feature. At lower heating beam energies, such as 2.0 μJ for the sombrero case, the growth of center peak reverses the slope sign if the location of the scanning He–Ne beam is fixed. Therefore, the deflection signal is reversed.

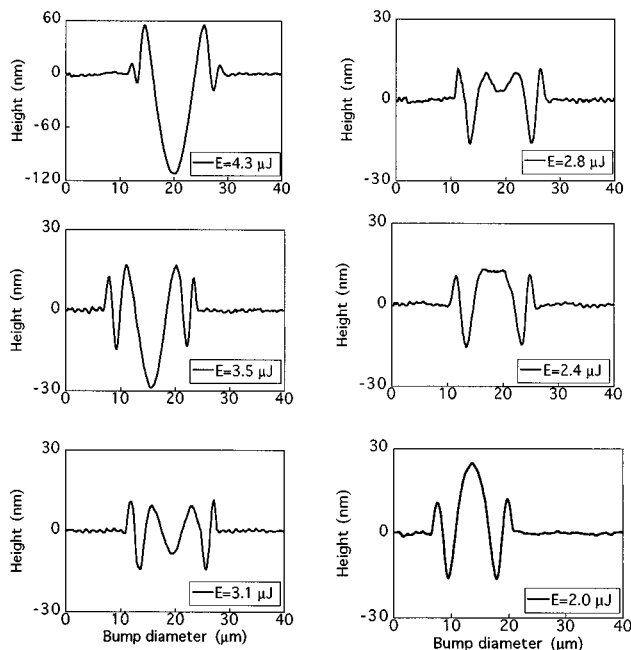


FIG. 5. Bump shape variation due to the incident heating beam energy change.

¹R. Ranjan, D. N. Lambeth, M. Tromel, P. Goglia, and Y. Li, *J. Appl. Phys.* **69**, 5745 (1991).
²D. Kuo, J. Gui, B. Marchon, S. Lee, *et al.*, *IEEE Trans. Magn.* **32**, 3753 (1996).
³P. Baumgart, D. J. Krajnovich, T. A. Nguyen, and A. C. Tam, *IEEE Trans. Magn.* **31**, 2946 (1995).
⁴T. D. Bennett, D. J. Krajnovich, C. P. Grigoropoulos, P. Baumgart, and A. C. Tam, *J. Heat Transfer* **119**, 589 (1997).
⁵A. C. Tam, I. K. Pour, T. A. Nguyen, D. J. Krajnovich, and P. Baumgart, *IEEE Trans. Magn.* **32**, 3771 (1996).
⁶H. K. Park, P. Kerstens, A. C. Tam, and P. Baumgart, *IEEE Trans. Magn.* **34**, 1807 (1998).
⁷*Photothermal Investigations of Solids and Fluids*, edited by J. A. Sell (Academic, New York, 1988).
⁸*Progress in Photothermal & Photoacoustic Science and Technology*, edited by A. Mandelis (Elsevier, New York, 1992), Vol. 1.
⁹N. M. Amer, *J. Phys. Colloq.* **C6**, 185 (1983).
¹⁰M. A. Olmstead, N. M. Amer, S. Kohn, *et al.*, *Appl. Phys. A: Solids Surf.* **32**, 141 (1983).
¹¹S. Chen and C. P. Grigoropoulos, *Appl. Phys. Lett.* **71**, 3191 (1997).
¹²J. Cheng, L. Wu, and S. Zhang, *J. Appl. Phys.* **76**, 716 (1994).